Metabolic Profiling during Peach Fruit Development and Ripening Reveals the Metabolic Networks That Underpin Each Developmental Stage[1][C][W]

Verónica A. Lombardo, Sonia Osorio, Julia Borsani, Martin A. Lauxmann, Claudia A. Bustamante, Claudio O. Budde, Carlos S. Andreo, María V. Lara, Alisdair R. Fernie, and María F. Drincovich*

Centro de Estudios Fotosintéticos y Bioquímicos, Facultad de Ciencias Bioquímicas y Farmacéuticas, Rosario 2000, Argentina (V.A.L., J.B., M.A.L., C.A.B., C.S.A., M.V.L., M.F.D.); Max-Planck-Institut für Molekulare Pflanzenphysiologie, 14476 Potsdam-Golm, Germany (S.O., A.R.F.); and Estación Experimental San Pedro, Instituto Nacional de Tecnología Agropecuaria, San Pedro 2930, Argentina (C.O.B.)

Fruit from rosaceous species collectively display a great variety of flavors and textures as well as a generally high content of nutritionally beneficial metabolites. However, relatively little analysis of metabolic networks in rosaceous fruit has been reported. Among rosaceous species, peach (*Prunus persica*) has stone fruits composed of a juicy mesocarp and lignified endocarp. Here, peach mesocarp metabolic networks were studied across development using metabolomics and analysis of key regulatory enzymes. Principal component analysis of peach metabolic composition revealed clear metabolic shifts from early through late development stages and subsequently during postharvest ripening. Early developmental stages were characterized by a substantial decrease in protein abundance and high levels of bioactive polyphenols and amino acids, which are substrates for the phenylpropanoid and lignin pathways during stone hardening. Sucrose levels showed a large increase during development, reflecting translocation from the leaf, while the importance of galactinol and raffinose is also inferred. Our study further suggests that posttranscriptional mechanisms are key for metabolic regulation at early stages. In contrast to early developmental stages, a decrease in amino acid levels is coupled to an induction of transcripts encoding amino acid and organic acid catabolic enzymes during ripening. These data are consistent with the mobilization of amino acids to support respiration. In addition, sucrose cycling, suggested by the parallel increase of transcripts encoding sucrose degradative and synthetic enzymes, appears to operate during postharvest ripening. When taken together, these data highlight singular metabolic programs for peach development and may allow the identification of key factors related to agronomic traits of this important crop species.

Rosaceae, comprising more than 100 genera and 3,000 species, is the third most economically important plant family in temperate regions of the world, with the genera *Malus*, *Pyrus*, and *Prunus* predominantly grown for their fruit (Dirlewanger et al., 2006; Shulaev et al., 2008). Fruits from Rosaceous species offer consumers a great variety of flavors, textures, and sweetness-acidity ratios. Moreover, rosaceous plants are extremely rich in specialized metabolites, many of which have recognized value in human health and nutrition, such as flavonoids, anthocyanins, and phenolics (Macheix et al., 1991; Swanson, 1998). *Prunus* has stone fruits or drupes in which seeds are covered by a hard, lignified endocarp (the stone), while the juicy mesocarp is the edible portion. Peach (*Prunus persica*) is one of the reference species for *Prunus* due to its high economic value, small genome size, taxonomic proximity to other important species, and availability of homozygous doubled haploids (Shulaev et al., 2008; Aranzana et al., 2010).

Fruit development and ripening are dynamic processes that involve a complex series of molecular and biochemical changes. The development process of stone fruits can generally be described as consisting of four clearly recognized distinct stages (S1–S4; Chalmers and van den Ende, 1975; Tonutti et al., 1997; El-Sharkawy et al., 2007). The first stage (S1), which is the first exponential growth phase, is characterized by a rapid increase in cell division and elongation. During the second stage (S2), the endocarp hardens to form the stone (pit hardening) and there is hardly any increase in fruit size (Dardick et al., 2010). In the third stage (S3), known as the second exponential growth phase, a rapid increase in fruit size takes place, along with rapid cell division. In the final stage (S4), the fruit reaches the final full size and enters the fruit ripening or climacteric stage. The S4 phase can be further subdivided into two phases: S4-1, in which the fruit arrives at its full size;

[1] This work was supported by the Argentine National Research Council (grant no. PIP 0679) and by the European Research Area net project TOMQML.

* Corresponding author; e-mail drincovich@cefobi-conicet.gov.ar.

The author responsible for distribution of materials integral to the findings presented in this article in accordance with the policy described in the Instructions for Authors (www.plantphysiol.org) is: María Fabiana Drincovich (drincovich@cefobi-conicet.gov.ar).

[C] Some figures in this article are displayed in color online but in black and white in the print edition.

[W] The online version of this article contains Web-only data.

www.plantphysiol.org/cgi/doi/10.1104/pp.111.186064

and S4-2, during which the fruit continues to ripen in an ethylene-dependent manner (Trainotti et al., 2003). The S4-2 stage can also take place in peach fruit detached from the tree and usually occurs prior to human consumption (Borsani et al., 2009).

During fruit development and ripening, the complex network of metabolites and proteins is dramatically altered. In this regard, metabolomics is an excellent tool for analyzing metabolism in developing fruit, due to its ability to follow a relatively large number of compounds in a single or a small number of analyses. Moreover, as the fruit is one of the most metabolite-rich organs of plants, it constitutes an excellent model for metabolomics studies. At present, most studies employing fruit metabolomics are focused mainly on tomato (*Solanum lycopersicum*; Roessner-Tunali et al., 2003; Carrari et al., 2006) and, more recently, on two nonclimacteric fruits, grape (*Vitis vinifera*; Deluc et al., 2007; Zamboni et al., 2010) and strawberry (*Fragaria* spp.; Fait et al., 2008; Osorio et al., 2011). Thus, it is essential to extend metabolomics to other fruit species. Moreover, broader use of metabolomics in Rosaceae will provide data sets that would help in modeling networks related to traits of agronomic interest as well as in the discovery of human health-promoting metabolites. In this study, metabolic profiling during peach development and ripening was assessed by gas chromatography-mass spectrometry (GC-MS), along with the analysis of key enzymes involved in carbon and nitrogen metabolism. These results allowed us to reveal what is to our knowledge the first high-resolution picture of the metabolic dynamics during peach development as well as to identify key enzymes associated with each peach developmental stage.

RESULTS

Dixiland Peach Fruit Development and Ripening

In order to characterize and identify the developmental stages of peach fruit (cv Dixiland), growth data were collected during at least three different years (2007, 2008, and 2009) by measuring fruit size along with fresh and dry weights. A typical growth profile with data collected during 2008, together with representative fruits from each developmental stage, are shown in Figure 1A. The peach cv Dixiland growth curve follows the double-sigmoid pattern that is characteristic of stone fruits (Chalmers and van den Ende, 1975). Dixiland peach fruit development was divided into four stages, S1 to S4, as described by Tonutti et al. (1991) for peach fruit cv Redhaven. Stage 1 (S1), from approximately 23 to 37 d after bloom (DAB), is characterized by fast fruit growth, with fruits increasing their volume more than three times in approximately 15 d (Fig. 1A). In stage 2 (S2), from approximately 38 to 66 DAB, the endocarp becomes lignified and the fruit growth is slow. Stage 3 (S3), from approximately 67 to 94 DAB, comprises the second fast increase in fruit size, increasing the fruit volume between three and four times in less than 30 d (Fig. 1A). Finally, stage 4 (S4), from 94 DAB, is the period when the fruit reaches its final full size and ripening takes place (Fig. 1A). In this work, the harvest of Dixiland peach was performed during S4 at approximately 102 DAB, when the fruit reached a flesh firmness of typically 57.1 $\pm$ 5.9 N (Borsani et al., 2009; Fig. 1A). After harvest, fruit was kept in a chamber at 20°C and 90% relative humidity for 7 d, a treatment that decreases the flesh firmness to values lower than 15 N. During this postharvest period (H–H7), the ripening process is similar to what occurs prior to human consumption (Borsani et al., 2009). Thus, under our growth conditions, the development of Dixiland peach fruit encompassed an average period of approximately 100 d, followed by a rapid ripening process that was accomplished in approximately 7 d.

Peach is a climacteric fruit, which significantly increases ethylene production during ripening. In higher plants, the final step of ethylene synthesis is catalyzed by the enzyme 1-aminocyclopropane-1-carboxylic acid oxidase (ACO). Previous work demonstrated that an accumulation of mRNA encoding peach ACO1 (*PpACO1*) correlates with the actual ethylene production by peach fruit (Tonutti et al., 1997; Ruperti et al., 2001; Borsani et al., 2009). Thus, in order to determine the onset and further progress of the ripening syndrome in Dixiland peach fruit, the *PpACO1* level was determined by quantitative real-time reverse transcription (qRT)-PCR during peach fruit development and ripening. *PpACO1* levels were relatively low and constant during almost all peach fruit development until the S4 stage, at which an approximately 10-fold increase was found (Fig. 1B). After harvest, a second 10-fold increase in *PpACO1* was detected concurrently with the ripening process (Fig. 1B). This *PpACO1* expression pattern agrees with previously reported results (Trainotti et al., 2007; Borsani et al., 2009) and allowed the identification of the transition from development to ripening in the Dixiland peach fruit.

The total protein relative to either fresh or dry weight ratio of peach fruits was also analyzed during development (Fig. 1C). In both cases, the protein-weight ratio was relatively high at the beginning of development (E) and decreased approximately 4-fold at S1. However, the main decrease in total protein content relative to dry or fresh weight (approximately 10-fold) took place between S1 and S2 (Fig. 1C). During subsequent developmental stages (S2–S4), as well as during postharvest ripening, no significant differences in the total protein-weight ratio were observed (Fig. 1C).

Metabolic Profiling during Peach Fruit Development and Ripening

In order to asses the metabolic profiles of peach fruit during development and ripening, representative peach samples were collected from the following

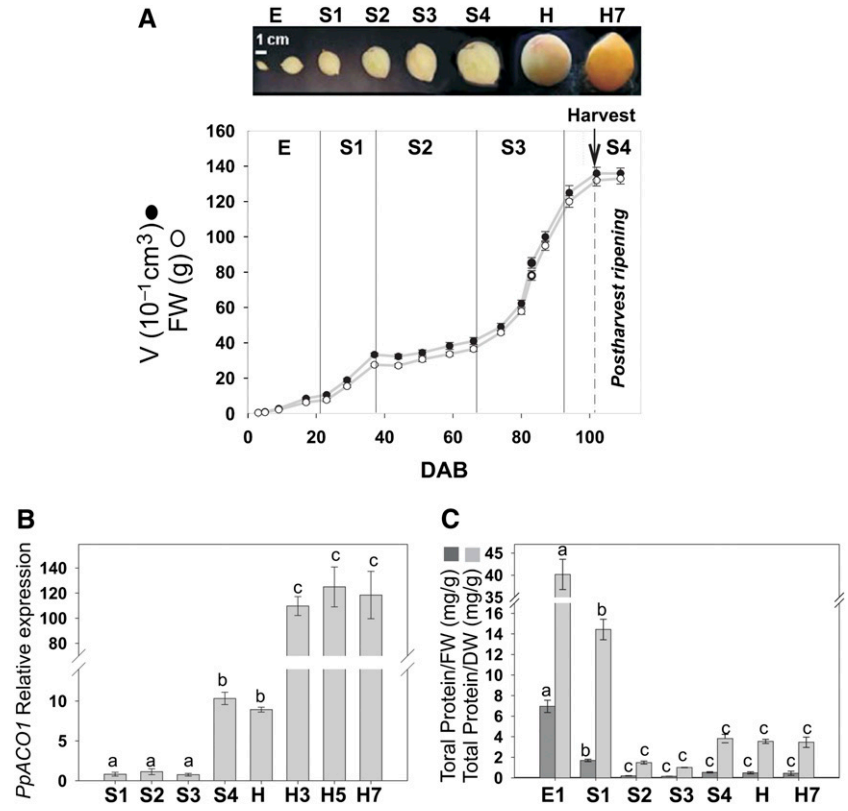

Figure 1. Dixiland peach fruits during development. A, Peach fruit growth curve. Volume (V) and fresh weight (FW) variations are shown for peach fruits collected during 2008 at early (E) fruit development (3, 5, 9, and 17 DAB) and stages S1 (23, 29, and 37 DAB), S2 (44, 51, 59, and 66 DAB), S3 (74, 80, 83, and 87 DAB), and S4 (94 and 102 DAB). Peach fruits were harvested at 102 DAB (H), as indicated by the arrow, and allowed to ripen at 20°C for 7 d (H7). A photograph of typical peach fruits at each developmental stage is shown in the top panel. B, *PpACO1* expression during peach fruit development. Peach fruits were collected at 29 (S1), 51 (S2), 80 (S3), 94 (S4), and 102 (H) DAB and at 3, 5, and 7 DAH (H3, H5, and H7, respectively), and *PpACO1* levels were analyzed by qRT-PCR. The means of the results obtained, using three independent RNAs as templates, are shown. Each reaction was normalized using cycle threshold (Ct) values corresponding to *EF1α* from peach. The *y* axis shows the fold difference in the *PpACO1* level relative to the amount found in peach fruits at S1. SD values are shown. Bars with the same letters are not significantly different ($P < 0.05$). C, Total protein level variation during peach fruit development. Total protein ratios relative to either dry weight (DW) or fresh weight (FW) during peach fruit development at 9 (E1), 29 (S1), 51 (S2), 80 (S3), 94 (S4), and 102 (H) DAB and 7 DAH (H7) are shown. Values represent means of 15 independent determinations using different fruits. SD values are shown. Bars with the same letters are not significantly different ($P < 0.05$). [See online article for color version of this figure.]

developmental stages during 2008: 9 and 17 DAB (E1 and E2, respectively) in early development; 35 DAB (S1) in the S1 stage; 59 DAB (S2) in the S2 stage; 83 DAB (S3) in the S3 stage; and 94 DAB (S4) corresponding to the S4 stage. Peach mesocarp was also collected from peach at harvest (102 DAB; H) and during the ripening process at 3, 5, and 7 d after harvest (DAH; H3, H5, and H7, respectively). Fifteen fruits at each developmental stage were collected, and five separate pools, each one composed of three different fruits, were used for metabolite extraction and subjected to GC-MS analysis to detect primary metabolite levels. By this technique, 47 metabolites were undoubtedly identified in peach cv Dixiland mesocarp and their levels relative to the ones detected at harvest (H) were measured (Supplemental Table S1).

Quantitative determination of the concentrations of 21 metabolites identified in peach cv Dixiland mesocarp was also performed by GC-MS analysis. A comparison of the absolute content (in $\mu g\ g^{-1}$ fresh weight) of each metabolite in fruits collected at harvest (H) time in three different years (2005, 2008, and 2010) is presented in Supplemental Table S2. In addition, the sorbitol content, determined by a spectrophotometric technique, is also included in Supplemental Table S2. Quantification of these metabolites indicates that the most abundant sugar in peach mesocarp is Glc, followed by Suc and Fru. With regard to organic acids, malate level is by far higher than that of citrate (Supplemental Table S2). Asp, Ser, and Glu are the amino acids that display the highest levels in peach mesocarp (Supplemental Table S2). When comparing

the absolute content of metabolites among the three years, the most significant changes were found in the absolute values of citrate, Fru, and Suc. However, the relative amounts among Fru, Glc, and Suc are practically in the same order of magnitude when comparing the three years. On the other hand, although citrate level varies among the three years, malate levels are in same order of magnitude and consistently significantly higher than citrate levels.

The data set obtained by GC-MS during development and ripening (Supplemental Table S1) was examined by principal component analysis (Fig. 2A), with two principal components explaining 76.9% of the overall variance of the metabolite profiles (53.1% and 23.8% for PC1 and PC2, respectively). This analysis highlights a clear metabolic shift among the first stages of development (E1–S1) to later developmental stages (S2–S4), when the fruit reaches its final size (Fig. 2A). Moreover, the ripening stages (H–H7) are grouped together but separate from the developmental stages (Fig. 2A).

Correlation analysis was also performed on the entire data set of metabolites during peach development and ripening. This analysis allows the identification of

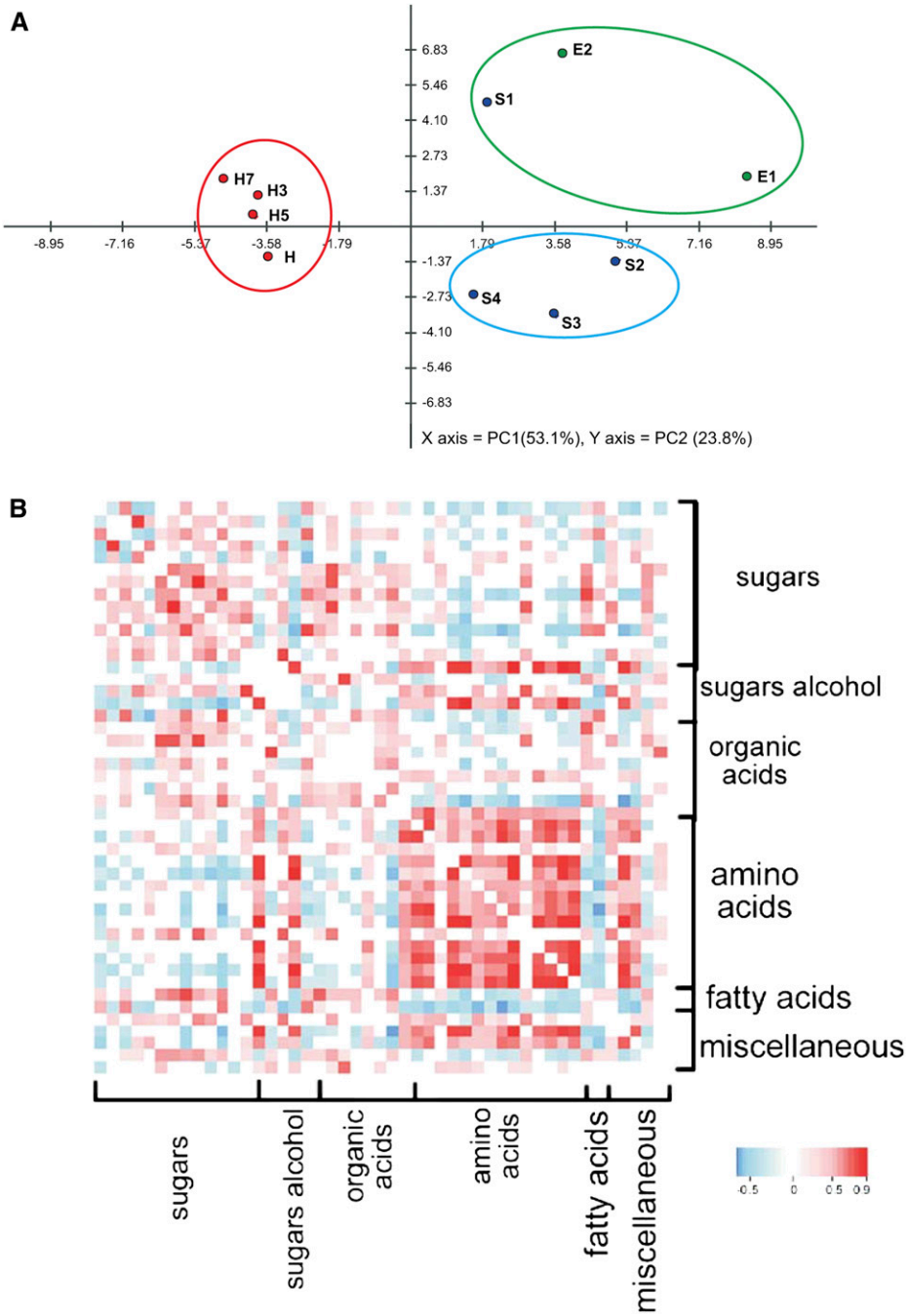

Figure 2. A, Principal component analysis of GC-MS data. Peach fruit samples from the following developmental stages were analyzed: early development (E1, 9 DAB; E2, 17 DAB); stages S1 (37 DAB), S2 (59 DAB), S3 (74 DAB), and S4 (87 DAB); harvest (H; 102 DAB); and during the postharvest ripening process at 3, 5, and 7 DAH (H3, H5, and H7, respectively). The variance explained by each component (%) is given in parentheses. Three separate groups can be easily distinguished: one encompassing E1, E2, and S1; another including S2 to S4; and a third including samples from the postharvest ripening process (H–H7). B, Visualization of metabolite-metabolite correlations during peach fruit development and ripening. Metabolites were grouped by compound class in the same order as shown in Supplemental Table S1. Correlation coefficients were calculated by applying Pearson correlation using R software. Out of 1,081 pairs of metabolites analyzed, 639 resulted in significant correlations ($P < 0.1$). From these, 425 were positive and 214 were negative. Each square represents the correlation between the metabolite heading the column and the metabolite heading the row with a false color scale (with color scale key at the bottom).

associations of metabolites across peach development and ripening, with a more detailed evaluation of the behavior of the metabolite network. Correlation analysis was carried out by the calculation of Pearson correlation coefficients for each metabolite pair as performed previously for other fruits (Carrari et al., 2006; Fait et al., 2008). Out of 1,081 total pairs analyzed, 639 resulted in significant correlation coefficients ($P < 0.1$). Out of these 639 significantly correlated, 425 were positive and 214 negative (Fig. 2B). Myoinositol-1-phosphate, amino acids (Glu, Val, Asp, Pro, Tyr, Ala, Phe, Thr, Gly, Iso, and Ser), galactinol, and caffeoylquinic acids showed by far the highest number of positive correlations (Fig. 2B). By contrast, Suc, malate, and urea correlate negatively with amino acids, myoinositol-1-phosphate, galactinol, and caffeoylquinic acids (Fig. 2B). Hexadecenoic and octadecanoic acids as well as the cell wall component Fuc also display negative associations with amino acids (Fig. 2B).

Metabolism of Sugars and Sugar Alcohols during Peach Fruit Development and Ripening

Sugars were the metabolites that displayed the most pronounced and continuous increase during development until harvest (Fig. 3; Supplemental Table S1). Suc, maltose, isomaltose, raffinose, and 1-*O*-methyl-glucoside increased during peach development (from E to H), with Suc displaying the highest rate of increase, approximately 50-fold from E to H (Figs. 3 and 4A). In the case of Xyl, raffinose, maltose, and isomaltose, a peak at S3 can be detected (Fig. 3). Glc, Fru, and glucoheptose also exhibited remarkable increases during peach development (Fig. 3). Trehalose levels increased at early developmental stages and were maintained thereafter. On the other hand, during postharvest ripening, sugar variances were not pronounced (Fig. 3), with the exception of a slight decrease in 1-*O*-methyl-glucoside and increases in Fuc, glucoheptose, and Fru-6-P at the late ripening stage (Fig. 3).

With regard to sugar alcohols, maltitol levels increased during development, from E2 until harvest, and were maintained thereafter (Fig. 3). Glycerol displayed a peak at harvest and decreased during postharvest ripening to the levels detected during development (Fig. 3). Myoinositol-1-phosphate and galactinol levels were highest at early stages of development, with a second peak at S3 in the case of galactinol (Fig. 3). In the case of myoinositol, a peak at S3 was also detected (Fig. 3). Considering sorbitol levels, a 3-fold increase was detected during the S2-to-S3 transition, and such levels were notably reduced during the ripening process (Fig. 4A).

As Suc and sorbitol are the main photosynthates translocated from leaves to fruits in Rosaceae, several enzymes involved in the metabolism of these com-

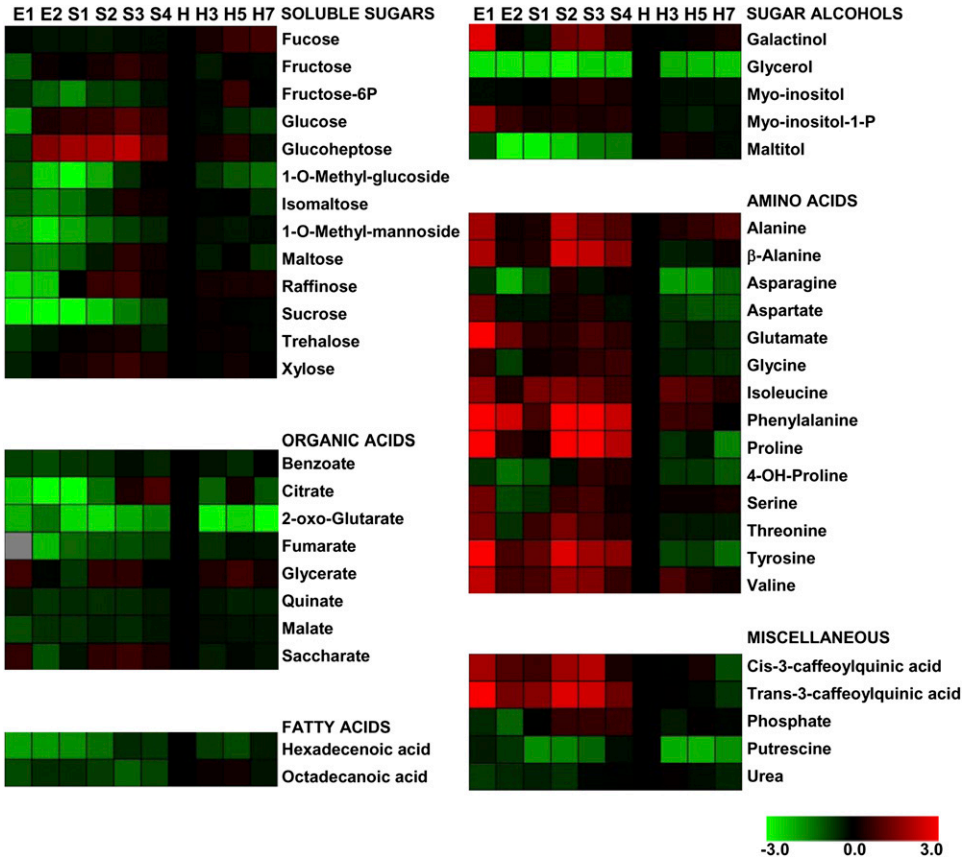

Figure 3. Distribution of metabolites analyzed by GC-MS during peach fruit development and ripening. The graph shows the relative level of each metabolite to its amount found in harvest peach fruit (H). Normalized values are shown on a color scale (shown at the bottom), which is proportional to the content of each identified metabolite. Mean values of five independent determinations for each stage were expressed as ratios between $\log_2$ and H using the MultiExperiment Viewer software (version 4.4.1; Saeed et al., 2003). The gray square indicates a value not determined. E1, 9 DAB; E2, 17 DAB; S1, 37 DAB; S2, 59 DAB; S3, 74 DAB; S4, 87 DAB; H, 102 DAB (harvest); H3, 3 DAH; H5, 5 DAH; H7, 7 DAH. Relative values for each metabolite peak area are provided in Supplemental Table S1.

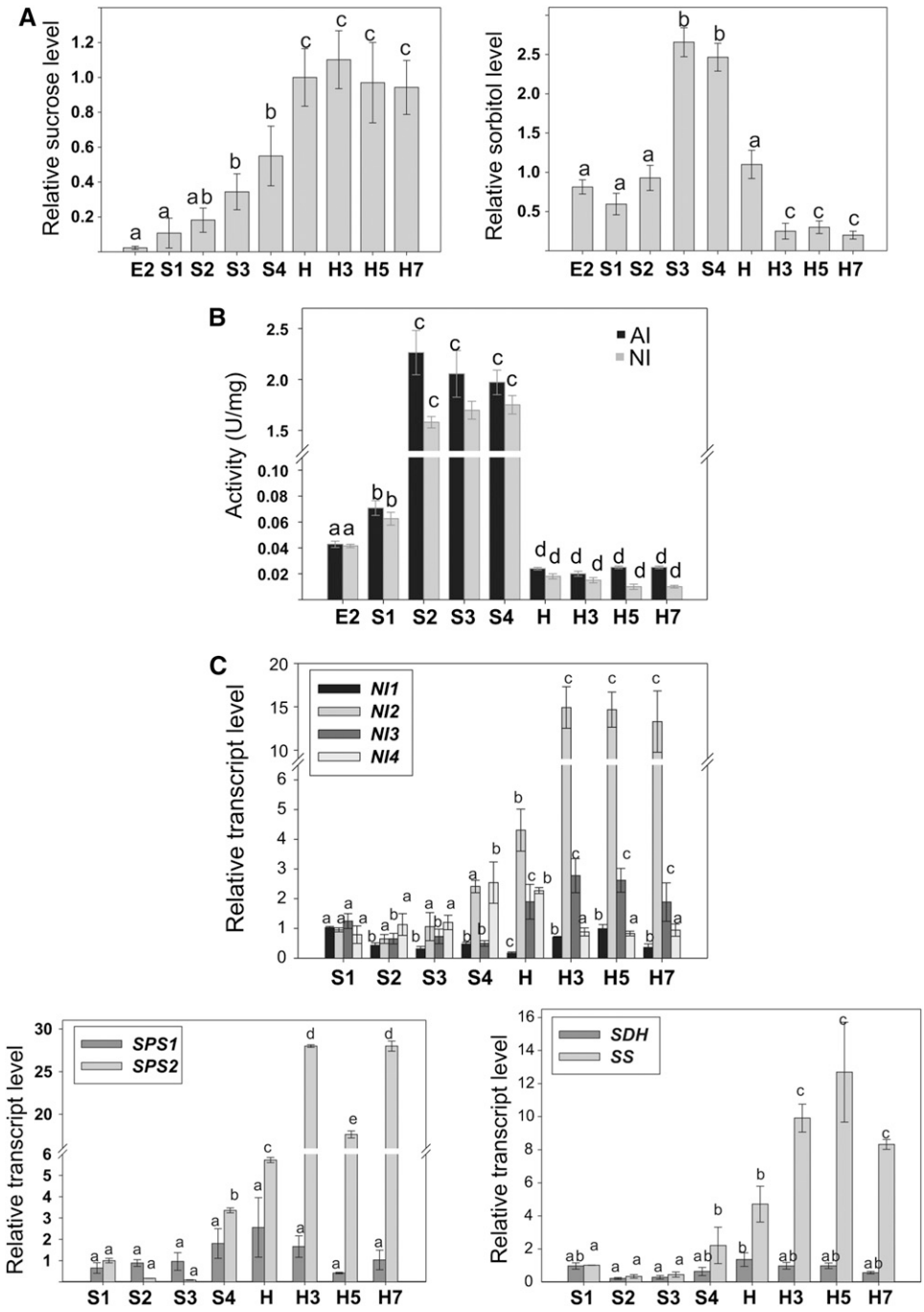

Figure 4. Sugar and sugar alcohol metabolism during peach fruit development and ripening. A, Suc and sorbitol levels during peach fruit development and ripening. Suc and sorbitol levels relative to the amount detected at harvest (H) are shown. Bars with the same letters are not significantly different ($P < 0.05$). B, AI and NI activities during peach fruit development and ripening. Activity is expressed in International Units per milligram of soluble protein (U/mg). Values represent means of at least 10 independent determinations in different peach fruits during development and postharvest ripening. For each enzyme, bars with the same letters are not significantly different ($P < 0.05$). C, Expression analyses of transcripts encoding enzymes involved in Suc (*NI1* to *-4*, *SS*, and *SPS1* and *-2*) or sorbitol (*SDH*) metabolism during peach fruit development and postharvest ripening. Means of results obtained, using three independent RNAs as templates, are shown. Each reaction was normalized using Ct values corresponding to *EF1α*. The *y* axes show the fold difference in a particular transcript level relative to its amount found in peach fruits at S1. SD values are shown. For each transcript analyzed, bars with the same letters are not significantly different ($P < 0.05$). E2, 17 DAB; S1, 37 DAB; S2, 59 DAB; S3, 74 DAB; S4, 87 DAB; H, 102 DAB (harvest); H3, 3 DAH; H5, 5 DAH; H7, 7 DAH.

pounds were analyzed by activity measurements and/or qRT-PCR (Fig. 4, B and C). Both acid invertase (AI) and neutral invertase (NI) activities highly increased during the S1-to-S2 transition (Fig. 4B). The increased invertase activity was maintained until the fruit reached its final size (S4). After harvest and during ripening, relatively lower invertase activities were maintained (Fig. 4B). Four putative NI transcripts, called *NI1* to *-4*, which were previously deduced from peach EST sequences (Borsani et al., 2009), displayed particular patterns of expression during peach development and ripening. Thus, while *NI2* increased approximately four times at harvest (from S1 to H) and a further 4-fold more during postharvest ripening with respect to H, *NI1* decreased approximately 2-fold at S2 in relation to S1, maintaining its levels practically constant thereafter (Fig. 4C). *NI3* decreased approximately two times at S2 in relation to S1 but increased between 2- and 3-fold at postharvest ripening, while *NI4* displayed a 2.5-fold peak at S4 and H with respect to S1 (Fig. 4C). Relative transcript levels for sucrose synthase (SS) were also analyzed during peach development and ripening. In this case, the lowest levels were detected from S1 to S3 and intermediate amounts

were measured in S4 and H, when a 4-fold increase was detected with respect to S1 (Fig. 4C). A second increase (approximately 2-fold) was detected during postharvest ripening at H3 with respect to H (Fig. 4C). Two putative sucrose phosphate synthase (*SPS*) transcripts, *SPS1* and *SPS2*, were also analyzed during peach development and ripening (Fig. 4C). While *SPS1* did not significantly change during peach fruit development and postharvest ripening, *SPS2* showed an approximately 6-fold increase during the S3-to-S4 transition (Fig. 4C). A further *SPS2* increase (approximately 5-fold with respect to H) was also detected during postharvest ripening (Fig. 4C). Finally, with regard to the sorbitol dehydrogenase transcript (*SDH*), no important changes were detected during either the development or postharvest ripening of Dixiland peach fruits (Fig. 4C).

Organic Acid Metabolism during Peach Fruit Development and Ripening

The pattern of levels for various organic acids measured during peach fruit development and ripening was diverse (Fig. 3). Citrate levels were relatively constant at the beginning of fruit development, showing a significant increase (approximately 10 times with respect to E2) at S4, followed by an approximately 2-fold decrease at harvest (H) with respect to S4 (Fig. 5A). The values measured at harvest were maintained during the whole postharvest ripening process (H3–H7; Figs. 3 and 5A). On the other hand, benzoate, fumarate, quinate, and malate levels did not significantly change during peach fruit development and ripening (Figs. 3 and 5A). With regard to 2-oxoglutarate levels, a peak at harvest was observed, followed by a decrease during ripening (Fig. 5A). Glycerate levels oscillated during peach development and ripening and were highest at E1, S2/S3, and H5 (Fig. 3). Saccharate content was modified during peach development and displayed a peak at E1 and S2/S3 (Fig. 3).

In addition, several key enzymes involved in organic acid metabolism were analyzed by activity measurement or qRT-PCR (Fig. 5, B and C). Activity of both NAD- and NADP- dependent malic enzymes (NAD-ME and NADP-ME, respectively) were measured (Fig. 5B). NAD-ME activity dropped approximately

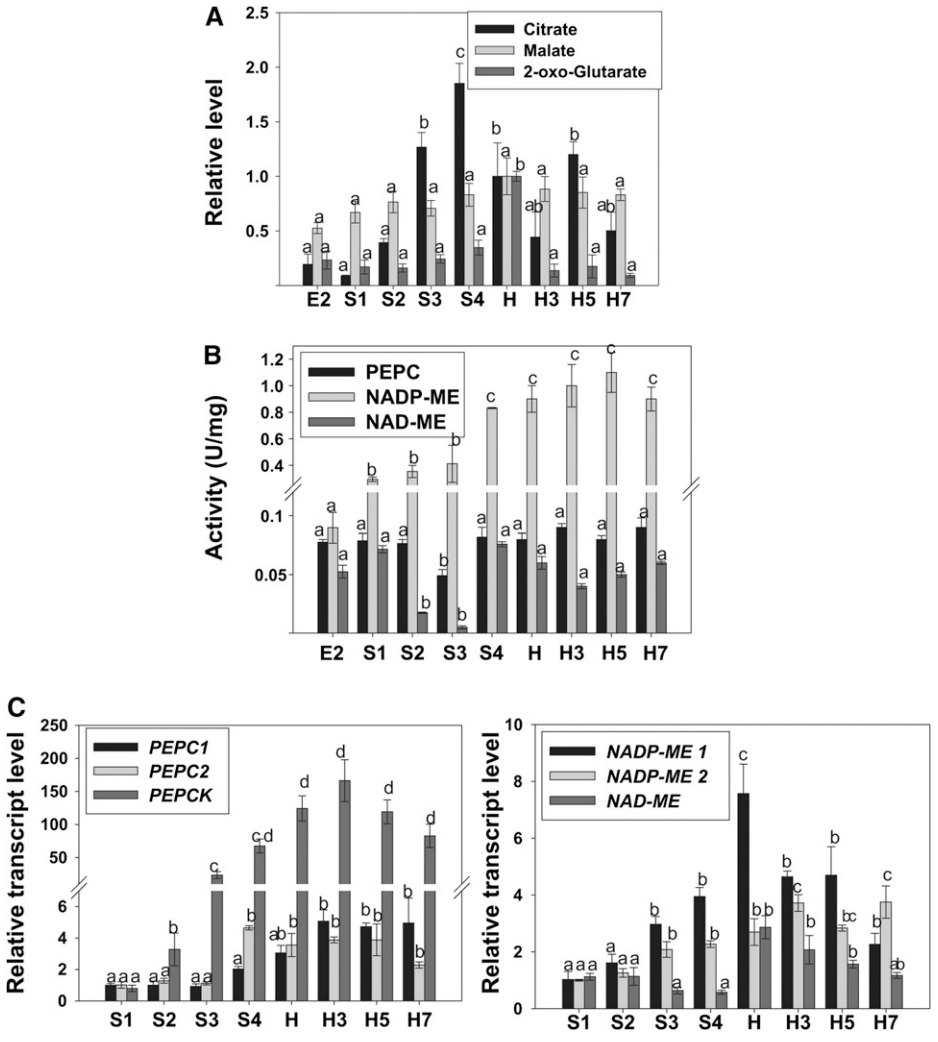

Figure 5. Organic acid metabolism during peach fruit development and ripening. A, Organic acid levels during peach fruit development and ripening. Citrate, malate, and 2-oxoglutarate levels relative to the amount detected at harvest analyzed by GC-MS are shown. Bars with the same letters are not significantly different ($P < 0.05$). B, Activity of enzymes involved in organic acid metabolism during peach fruit development and postharvest ripening. Activity is expressed in International Units per milligram of soluble protein (U/mg). Values represent means of at least 10 independent determinations in different peach fruits during development and postharvest ripening. For each enzyme, bars with the same letters are not significantly different ($P < 0.05$). C, Expression analyses of transcripts encoding enzymes involved in organic acid metabolism during peach fruit development. Means of results obtained, using three independent RNAs as templates, are shown. Each reaction was normalized using Ct values corresponding to *EF1α*. The *y* axes show the fold difference in a particular transcript level relative to its amount found in peach fruits at S1. SD values are shown. For each transcript analyzed, bars with the same letters are not significantly different ($P < 0.05$). E2, 17 DAB; S1, 37 DAB; S2, 59 DAB; S3, 74 DAB; S4, 87 DAB; H, 102 DAB (harvest); H3, 3 DAH; H5, 5 DAH; H7, 7 DAH.

4-fold during the S1-to-S2 transition, with a subsequent return to levels detected at S1 during the S3-to-S4 transition (Fig. 5B). In the course of the postharvest ripening, the activity detected at the S4 stage was maintained (Fig. 5B). With regard to NADP-ME, two statistically significant increases during peach fruit development, one of 3-fold at S1 with respect to E2 and the other of 2-fold during the S3-to-S4 transition, were detected (Fig. 5B). This high NADP-ME activity was maintained at harvest and during postharvest ripening (Fig. 5B). Another enzyme analyzed was phospho*enol*pyruvate carboxylase (PEPC), which showed no statistically significant changes during peach fruit development and ripening, with the exception of a transitory and slight decrease at S3 stage (Fig. 5B). Regarding the levels of transcripts encoding different enzymes involved in organic acid metabolism, *NAD-ME* levels did not show any statistically significant differences during peach fruit development (Fig. 5C). However, at harvest and during postharvest ripening, higher levels of this transcript were found (Fig. 5C). Two different transcripts encoding NADP-ME, *NADP-ME1* and *NADP-ME2*, were also analyzed. *NADP-ME1* increased during peach development, showed the highest levels at harvest, and decreased during the postharvest ripening process to values similar to those of S3 and S4 (Fig. 5C). In relation to *NADP-ME2*, a continuous increase was detected, with the lowest levels at S1/S2, intermediate levels at S3/H, and highest levels at H3 to H7 (Fig. 5C). Two putative *PEPC* transcripts, *PEPC1* and *PEPC2*, were also analyzed, both with increased levels during development, 2-fold in the case of *PEPC1* and 4-fold in the case of *PEPC2* at the S3-to-S4 transition, and maintained thereafter (Fig. 5C). Finally, the levels of a transcript encoding phospho*enol*pyruvate carboxykinase (PEPCK) increased significantly during peach fruit development, with levels approximately 50 times higher at S4 with respect to S1 (Fig. 5C). Moreover, higher *PEPCK* levels (between 100 and 150 times) with respect to S1 were detected during the postharvest ripening process (Fig. 5C).

Metabolism of Nitrogen-Containing Compounds during Peach Fruit Development and Ripening

Out of the 14 amino acids detected by GC-MS during peach fruit development, 12 dramatically decreased during early development (Fig. 3; Supplemental Table S1). Pro was the amino acid that displayed the highest rate of decrease at the E1-to-E2 transition (approximately 17-fold), followed by Tyr (approximately 9-fold), Thr and Ser (approximately 4-fold), and Gly, Ala, β-Ala, Asp, Asn, Glu, Val, and Ile (approximately 3-fold; Fig. 3). Some amino acids, such as Ala, β-Ala, Ile, Phe, Pro, Val, and Tyr, displayed an increase at S2 (Fig. 3). An overall decrease in the levels of the amino acids detected was observed during ripening, with Asn displaying an approximately 5-fold decrease (Fig. 3).

The relative expression of transcripts encoding some key enzymes involved in nitrogen metabolism was also analyzed (Fig. 6B). The level of the transcript encoding glutamine synthetase (*GS*) did not significantly change during development; however, a significant increase was observed in this transcript during postharvest ripening, with an approximately 10-fold increase at H3 and H5 with respect to S1 (Fig. 6B). In addition, the relative expression of transcripts encoding glutamate dehydrogenase (*GDH*) and asparaginase (*ASE*) was also analyzed during peach development and ripening (Fig. 6B). An increase in *GDH* was observed at the final development stage (S4) and harvest with respect to the first stages (S1–S3), and these higher levels were maintained during postharvest

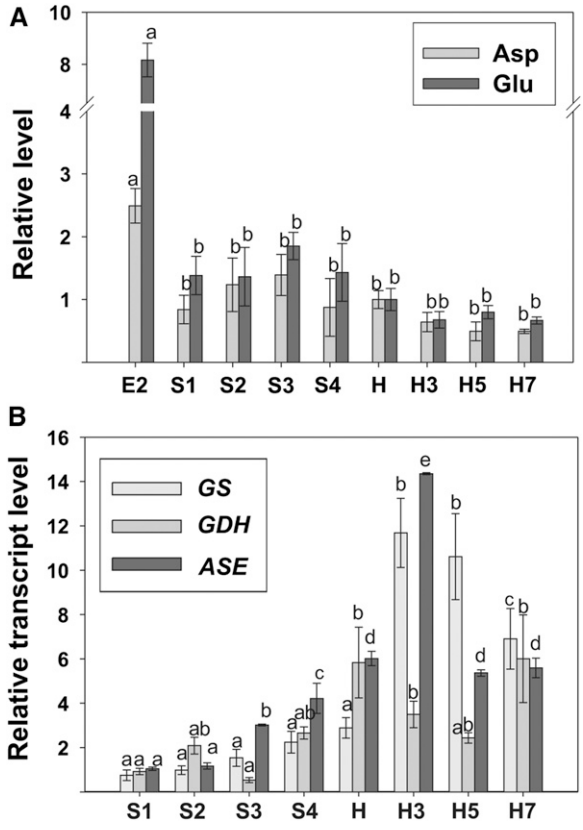

Figure 6. Amino acid metabolism during peach fruit development and ripening. A, Amino acid levels during peach fruit development and postharvest ripening. Relative Glu and Asp levels (to the amount detected at harvest) analyzed by GC-MS are shown. Bars with the same letters are not significantly different ($P < 0.05$). B, Expression analyses of transcripts encoding enzymes involved in amino acid metabolism during peach fruit development and postharvest ripening. Means of results obtained, using three independent RNAs as templates, are shown. Each reaction was normalized using Ct values corresponding to *EF1α*. The *y* axes show the fold difference in a particular transcript level relative to its amount found in peach fruits at S1. SD values are shown. For each transcript analyzed, bars with the same letters are not significantly different ($P < 0.05$). E2, 17 DAB; S1, 37 DAB; S2, 59 DAB; S3, 74 DAB; S4, 87 DAB; H, 102 DAB (harvest); H3, 3 DAH; H5, 5 DAH; H7, 7 DAH.

ripening (Fig. 6B). Finally, with regard to *ASE*, a gradual increase was detected during development, with levels approximately six times higher at harvest in relation to the level detected at S1 (Fig. 6B). A further increase in *ASE* was detected at H3 (more than two times with respect to H), followed by a decrease to the levels measured at harvest (Fig. 6B).

Fatty Acid, Caffeoylquinic Acid, and Putrescine Levels during Peach Fruit Development and Postharvest Ripening

Hexadecenoic and octadecanoic acids were also analyzed during peach fruit development and ripening (Fig. 3). Both fatty acids displayed significant increases during peach development until harvest (Fig. 3). Both trans- and cis-3-caffeoylquinic acids, which are derived from the phenylpropanoid pathway, displayed their highest levels during early peach fruit development, maintained high levels during development (with a peak at S2/S3), and decreased during postharvest ripening, reaching their lowest levels at the last postharvest ripening state, H7 (Fig. 3; Supplemental Table S1).

Putrescine levels, which were lower at S1 and S2 with respect to the first stages (E1 and E2), increased at harvest and significantly decreased thereafter, during postharvest ripening (Fig. 3; Supplemental Table S1). Finally, phosphate levels were highest at late developmental stages (S2–S4) and slightly decreased at harvest and during the postharvest ripening stages (Fig. 3).

DISCUSSION

Metabolic profiling has been successfully applied to study the development of three important crop fruits: tomato (Roessner-Tunali et al., 2003; Carrari et al., 2006), strawberry (Fait et al., 2008), and grape (Deluc et al., 2007; Zamboni et al., 2010). These three species constitute distinct model fruits, not only at the physiological level but also at the biochemical level. Tomato fruit is a climacteric berry, with a peel tissue enclosing a fleshy pericarp and seeds. On the other hand, grape and strawberry are both nonclimacteric fruits, but significantly different at the physiological level. Grape is a typical berry, in which the entire ovary wall ripens into an edible pericarp. By contrast, strawberry is a so-called false fruit, with a fleshy receptacle tissue and the achenes on the surface. While in climacteric fruits, autocatalytic ethylene synthesis is required to complete ripening, nonclimacteric fruits do not exhibit the climacteric ethylene peak (Giovannoni, 2004). In this work, metabolomics was applied to the analysis of peach fruit. Peach represents a novel model fruit in terms of physiology, anatomy, and metabolism, different from tomato, strawberry, or grape since it is a drupe, with seeds covered by a lignified endocarp and a juicy mesocarp. Although peach is a climacteric fruit, other hormones may also be involved in the ripening process (Trainotti et al., 2007).

Metabolism during Early Stages of Dixiland Peach Fruit Development Supports Fruit Growth and Stone Formation

The early developmental stages, E to S3, comprise the peach fruit size growth period (Fig. 1). During this phase, the growth plateau at S2 matches the stone lignification process (Dardick et al., 2010). The lowest *PpACO1* levels were detected at these stages (Fig. 1B), although the changes that take place (fruit growth and stone hardening) are ethylene independent (Fig. 7).

Total protein levels in peach were highest at E and significantly decreased at S1 and S2 (Fig. 1C). Thus, it is clear that immature peach fruits store high levels of proteins, which are mainly used for the processes that occur at S1 and S2 (Fig. 7). The metabolic profiling also indicates high levels of several amino acids, such as Pro, Phe, Tyr, and Glu, at E1, most of which significantly decrease at E2 (Fig. 3; Supplemental Table S1). However, an important peak at S2/S3 was found for particular amino acids, such as Phe, Pro, Tyr, Ala, and Val, with Phe reaching even higher levels than those found at E1 (Fig. 3). In this scenario, it is highly probable that amino acids derived from stored proteins in the early immature fruit become the substrates for the phenylpropanoid, lignin, and flavonoid pathways that are induced concomitantly with the deposition of lignin in the stone at S2 (Fig. 7; Dardick et al., 2010). Moreover, the high levels of the caffeoylquinic acids measured during early peach development (Fig. 3) are in accord with an induction of the mentioned metabolic pathways during pit hardening (Fig. 7). Caffeoylquinic acid represents an important group of plant-based bioactive polyphenols with significant antioxidant activity, which has been reported as having an important beneficial effect in human health (Luo et al., 2008).

With regard to sugars, very low levels were found at the earliest developmental stage, E1 (Fig. 3). Suc, Glc, and Fru levels highly increase from E1 to S3 (approximately 17-, 13-, and 3-fold, respectively). The rise in Suc may be due to photosynthate translocation from the leaf, where it is loaded into the phloem in either an apoplastic or a symplastic manner (Moing et al., 1997; Lo Bianco et al., 1999, Nadwodnik and Lohaus, 2008). Moreover, the marked increase in invertase activity at S2 to S4 (Fig. 4B) would probably favor a high rate of Suc unloading into the fruit during these stages (Fig. 7; Fridman et al., 2004). In addition, the further hydrolysis of Suc to Glc and Fru may provide the necessary energy to sustain both fruit growth and stone formation through the highly energy-consuming pathways induced at S2 (Fig. 7). Surprisingly, the increase in NI activities at S2 to S4 did not correlate with the increase in any particular *NI* transcript, except for the observed increase in *NI4* at S4 (Fig. 4C). Thus, a translational or posttranslational process regulating invertase activity may well be involved at these early stages. In this

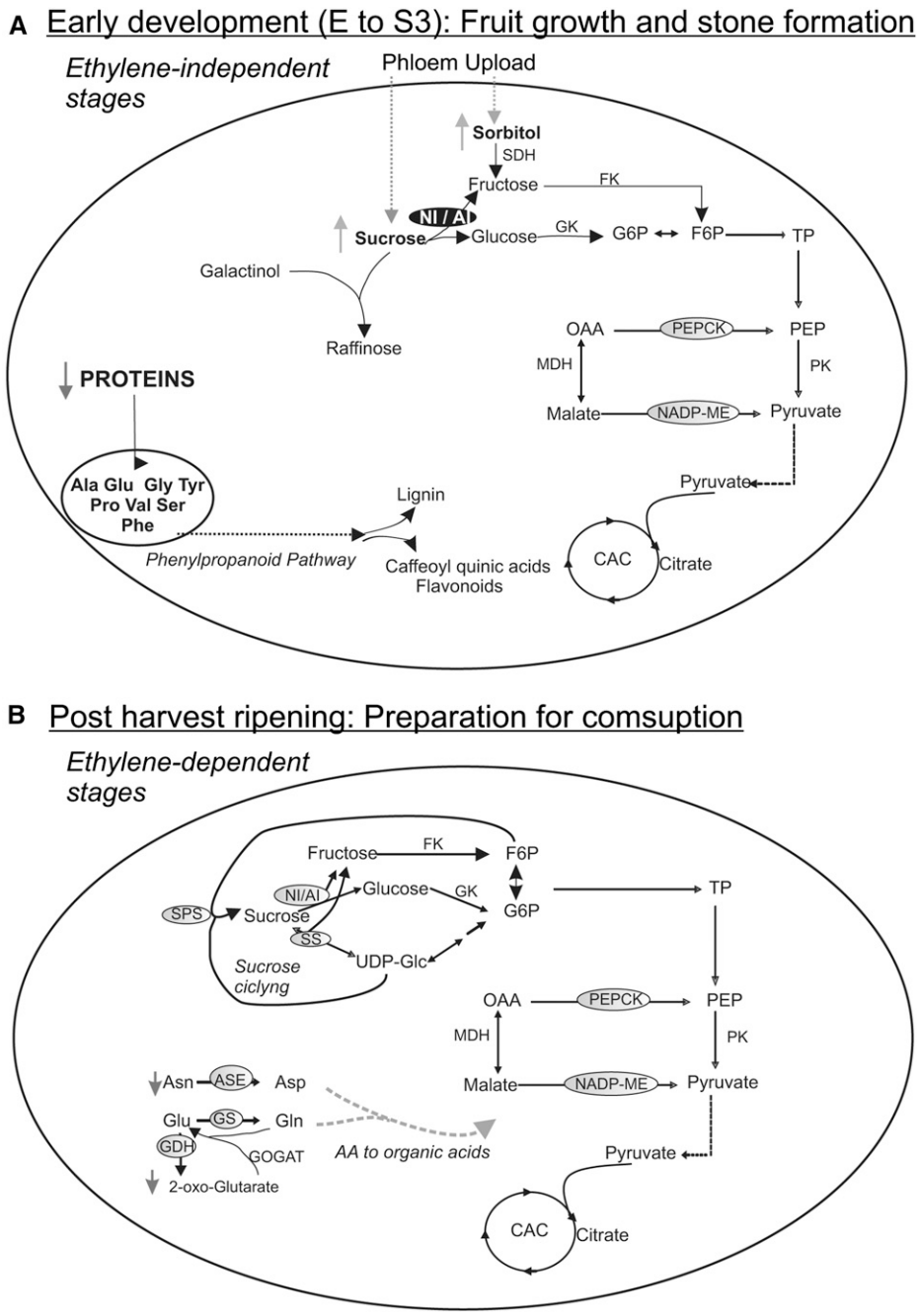

Figure 7. Simplified scheme of key metabolic processes occurring during early development (A) and postharvest ripening (B) of Dixiland peach fruit. The scheme highlights key metabolic processes during the development or ripening of peach fruit. Metabolites indicated with up arrows or down arrows increased or decreased, respectively, during each particular stage. Invertase (NI/AI) is particularly prominent in A due to its high activity at early developmental stages. CAC, Citric acid cycle; FK, fructokinase; F6P, Fru-6-P; GK, glucokinase; G6P, Glc-6-P; OAA, oxaloacetate; TP, triose phosphate.

regard, the tight regulation of tomato invertase activity by a specific invertase inhibitor protein (Jin et al., 2009) could also take place in peach.

Considering sugar alcohols, an increase in sorbitol levels was found in S3 compared with E2 (Fig. 4A), which was not accompanied by changes in *SDH* levels (Fig. 4C). Since sorbitol, together with Suc, is transported from leaves to fruits in Rosaceae, higher levels of this metabolite may be a consequence of greater import due to higher sink strength at this stage of development (Fig. 7; Moing et al., 1997; Nadwodnik and Lohaus, 2008).

The results regarding the other sugar alcohols analyzed, mainly galactinol, myoinositol, and raffinose, are rather surprising. High levels of galactinol and myoinositol-1-phosphate were detected at E1; myoinositol-1-phosphate further decreased from E1 to S3 in parallel with a 10-fold increase in raffinose, along with the occurrence of a second peak of galactinol in S2/S3 (Fig. 3). Thus, high levels of galactinol and raffinose were observed during pit hardening. Galactinol (galactopyranosyl-myoinositol) is synthesized from UDP-Gal and myoinositol and used as the galactosyl donor, while Suc is the acceptor for the synthesis of the

trisaccharide raffinose. Raffinose is one of the main oligosaccharides constituting a significant component of phloem-transported sugars in certain species such as cucurbit plants. Besides being translocated, raffinose concentrations in the fruit flesh of watermelon (*Citrullis vulgaris*) are negligible, due to its hydrolysis while being unloaded (Yativ et al., 2010). In contrast, the accumulation of raffinose oligosaccharides has been associated with stressful environmental conditions (Taji et al., 2002). More importantly, the potential role of these oligosaccharides has been intensively studied in seeds, where their accumulation coincides with the development of desiccation tolerance during seed maturation (Horbowicz and Obendorf, 1994; Lin and Huang, 1994; Bernal-Lugo and Leopold, 1995). Besides, these oligosaccharides have also been suggested to accumulate in seeds as a readily metabolizable carbohydrate source for energy generation during germination (Downie and Bewley, 2000). Thus, the simultaneous occurrence of the high galactinol and raffinose levels along with stone formation suggests an important role of these compounds in peach seed formation. To our knowledge, this is the first time that raffinose has been detected in peach fruits and that a link between this trisaccharide and stone formation or seed maturation has been suggested (Fig. 7).

The three main organic acids in the peach fruit, citrate, malate, and quinate, have been suggested to undergo continuous accumulation during fruit development for their further respiratory consumption (Moing et al., 1998; Etienne et al., 2002). In this work, the metabolic profiling of Dixiland peach showed practically constant levels of quinate and malate during the E to S4 stages (Figs. 3 and 5A). Significant increases in both NADP-ME activity and *NADP-ME1* and -2 were found during peach development (Fig. 5, B and C). Moreover, while *PEPCK* levels were highly increased at S3 in relation to S1 (Fig. 5C), PEPC activity was reduced in S3 with respect to E (Fig. 5B). Thus, both NADP-ME and PEPCK, functioning as decarboxylating enzymes, may be involved in organic acid catabolism at early development stages and, thereby, prevent malate accumulation (Fig. 7). The important decrease in free amino acid content during the early stages as well as the higher levels of citrate, compared with E, detected at S3 (Figs. 3 and 5A) are the grounds for our hypothesis concerning amino acid metabolization into organic acids at this stage (Fig. 7). In addition, it is interesting that increased NADP-ME activity at an early stage (S1) could provide NADPH for lignin, phenylpropanoid, and flavonoid synthesis during pit hardening.

Metabolism during Late Maturation of Dixiland Peach Fruit: Reaching Final Size and Preparing for Ripening

At late developmental stages in peach (S4 and H), the fruit reaches its final size attached to the tree (Fig. 1A). During this period, the first increase in *PpACO1* was observed (Fig. 1B). As *PpACO1* levels are highly correlated with the rate of ethylene release (Tonutti et al., 1997; Ruperti et al., 2001; Borsani et al., 2009), an increase in ethylene production is occurring at this stage. It is then possible that such an increase would trigger the remarkable ethylene increase detected during postharvest ripening (Fig. 1B; Borsani et al., 2009).

During the transition from S4 to H, amino acid levels (such as Phe, Pro, Tyr, and Ala) were still high compared with earlier stages, although significant reductions were observed (Fig. 3). As the lignification process is considered complete at this stage, it is most likely that amino acids would be used as either energy fuels or precursors for flavonoid synthesis. The increase in *GDH* and *ASE* in relation to early developmental stages (Fig. 6B) is in accord with the catabolism of amino acids into organic acids for fuel. Moreover, a decrease in citrate level along with an increase in 2-oxoglutarate, which reaches the highest level at H (Figs. 3 and 5A), were detected. The peak in *NADP-ME1* and the corresponding increase in activity at H, together with an increase in *PEPCK* levels (Fig. 5C), are in agreement with the suggested catabolism of amino acids to provide organic acids to fuel respiration, as has previously been reported during dark-induced senescence (Ishizaki et al., 2006; Araújo et al., 2010) and overexpression of amino acid transporters (Weigelt et al., 2008).

An increase in Suc content was also detected at the transition from S4 to H (Figs. 3 and 4A), when the delivery of this disaccharide is halted due to fruit separation from the tree. In accordance with this observation, a dramatic decrease (approximately 20 times) in invertase activity was detected at this point (Fig. 4B), which is consistent with a role of invertase in the facilitation of Suc unloading from the phloem into the fruit. Again, the decrease in NI activity was not correlated to any particular *NI* (Fig. 4C). The sorbitol level peaked at S4 and decreased by 50% at H (Fig. 4A). This result suggests a rapid mobilization of this sugar alcohol, which it is not a major storage form of carbon in the fruit, despite being a major form of carbon transport from leaf to fruit in Rosaceae.

Metabolism during Ripening of Dixiland Peach Fruit: Preparing for Consumption

During the postharvest ripening process, the peach fruit is transformed into a palatable product for consumers (Borsani et al., 2009). All these modifications affect the nutritional quality, flavor, and aroma, and the ratio between sugars and organic acids at the ripe state contributes significantly to the overall flavor of the fruit. The changes that occur in peach at this stage are related to ethylene synthesis, as accounted for by the approximately 100-fold *PpACO1* increase in relation to early stages (Fig. 1B).

Contrary to the early stages of development, which are characterized by high levels of amino acids, the majority of these compounds decreased during ripening (Fig. 3). Such is the case for Asn and Tyr, which

decreased approximately 3- and 2-fold in relation to H, respectively (Fig. 3). These data, together with the high increase of the transcripts encoding major enzymes involved in amino acid catabolism (*ASE*, *GDH*, and *GS*) typical of the postharvest stage (Fig. 6B), indicate that amino acids are used as respiratory substrates during the ripening process (Fig. 7). Furthermore, the high levels of NADP-ME activity, and *NADP-ME1* and *PEPCK* transcripts during the ripening process (Fig. 5, B and C), support this theory (Fig. 7), particularly considering that a role for PEPCK in organic acid catabolism in certain fleshy fruits has been suggested previously during ripening (Famiani et al., 2005).

Putrescine levels were significantly reduced during postharvest ripening (Fig. 3). Putrescine is a polyamine that has been implicated in a wide range of developmental processes. The decrease found during postharvest ripening is in accordance with previous results (Ziosi et al., 2009) and with the potential role of polyamine as a senescence inhibitor. Therefore, low levels of putrescine and a high release of ethylene would favor the postharvest onset of the senescence process.

With regard to sugars, almost constant Suc levels were found throughout the ripening process (Figs. 3 and 4A). Suc degradation can take place via SS to hexose phosphate or via invertase, while SPS is a key enzyme involved in Suc synthesis (Fig. 7). Although invertase activity (both AI and NI) remained low during peach postharvest ripening in relation to early stages (Fig. 4B), specific induction of distinct putative NI transcripts was detected (a remarkably 7-fold increase in *NI2*). Thus, no correlation was found between invertase transcript level and activity, which may be due to translational or posttranslational regulation of invertase activity. Nevertheless, the particular response of each *NI* during peach development and different postharvest treatments (Lara et al., 2009, 2011) indicates that NI transcripts display particular roles that will require further analyses. This hypothesis is reinforced by the discovery of novel physiological functions (Roitsch and González, 2004) and compartmentalization of invertases (Vargas et al., 2008; Vargas and Salerno, 2010). On the other hand, an increase in *SS* and *SPS2* levels was also detected during postharvest peach ripening (Fig. 4C). The parallel increases in transcripts involved in Suc degradation (*NI2* and *-3* and *SS*) and synthesis (*SPS2*) suggest a cycle for both processes (Fig. 7), as was observed during anoxia treatment of peach fruit (Lara et al., 2011). Such Suc cycling has also been detected in many other tissues, where it was suggested to control several important physiological functions (Roby et al., 2002; van der Merwe et al., 2010). The particular role of such a cycle during peach ripening will require detailed analysis in the future. That said, the increases in both degradative and synthetic Suc pathways are in keeping with the unchanged levels of this metabolite (Fig. 3A). Finally, regarding sorbitol, a dramatic decrease was found during the ripening process (Fig. 4A), supporting previous suggestions (Borsani et al., 2009) that this sugar alcohol is no longer used as carbon fuel at 3 DAH.

Fruit Development in Peach Is a Process Metabolically Different from Those Operating in Other Model Fruits: Identification of Key Metabolic Steps in Peach

The comparison of metabolic profiling during the development of peach and other fruits indicates that each fruit follows a diverse metabolic program. For example, dramatic differences were detected in the case of tomato, where some amino acids increased while others decreased at early developmental stages and Suc levels decreased during development (Carrari and Fernie, 2006; Carrari et al., 2006). However, it seems that invertase displays a central role in tomato as well as in peach (Fridman et al., 2004; Zanor et al., 2009). On the other hand, and similar to what can be observed in peach, an increase in the content of certain amino acids was found during strawberry achene development. However, it was suggested that this increase would be due to amino acid import from the mother plant (Fait et al., 2008). Finally, in the case of grape berries, Suc was relatively low and constant during berry development (Deluc et al., 2007), in contrast to the important increase found in peach. Since great differences in terms of morphology are found among fruits, it seems reasonable that singular metabolic programs support the differential developmental processes.

Figure 7 summarizes the most relevant metabolic steps during peach development and ripening derived from this work. The principal roles of stored proteins and amino acid metabolism during early stages (as substrates for the phenylpropanoid pathway) and also during ripening (as fuels) are highlighted, an observation that was not reported previously in the case of peach. Thus, enzymes involved in amino acid metabolism may be useful biomarkers for the different developmental stages as well as key in determining the final quality of the peach fruit. On the other hand, metabolic determinants for Suc levels, invertase activity for early stages and Suc cycling for ripening, are also inferred from this work. The relevance of stone formation by lignification of the fruit endocarp layer, which affects primary metabolism to fulfill this process, is also remarked. Lignin is a compound of tremendous economic importance that is unique to plants and has been found at extremely high levels in peach stones (Dardick et al., 2010). Although the metabolic programs to sustain the lignification process may vary among the different species with stone fruits, key processes in the biosynthesis of substrates for the phenylpropanoid pathway were identified in this work for peach. Finally, the relevance of the posttranscriptional regulation of enzyme activity is also inferred from this study, indicating the need for integrated studies of metabolic pathways, combining analyses of metabolite, transcript, protein, and enzyme activity levels.

MATERIALS AND METHODS

Plant Material

Assays were conducted using peach fruit (*Prunus persica* 'Dixiland') grown in the Estación Experimental Agropecuaria, San Pedro, Argentina (Budde et al., 2006; Borsani et al., 2009). Fruit growth was monitored weekly on at least 10 fruits by measuring the increase in volume and fresh weight of fruits collected at different development stages. Volume calculation was carried out through the volume sphere equation using the average radius of fruits at different DAB. Dry and fresh weight determinations were carried out by weighing peach fruits at different developmental stages in fresh fruit and after incubation at 80°C up to constant weight. Early fruit development samples (E) were collected at 3, 5, 9 (E1), and 17 (E2) DAB. Fruit samples were collected at the S1 stage (23, 29, and 37 DAB), the S2 stage (44, 51, 59, and 66 DAB), the S3 stage (74, 80, 83, and 87 DAB), and the S4 stage (94 and 102 DAB). Peach samples were also collected at harvest when the fruit reached a flesh firmness of typically 57.1 ± 5.9 N (Borsani et al., 2009), at approximately 102 DAB. After harvest, fruits were kept in a chamber at 20°C and 90% relative humidity for 7 d, when fruit flesh firmness reached values lower than 15 N (Borsani et al., 2009). Samples were collected after 3, 5, and 7 DAH and named as H3, H5, and H7, respectively. Whole fruit tissue was used for samples taken during E, as the seed is inseparable; while for S1, S2, S3, and S4 stages, representative mesocarp tissue was collected. At least 20 fruits at each developmental stage were collected. Five separate pools, each one composed of three different fruits of the same developmental stage, were used for further analysis. Samples were immediately frozen in liquid N_2 and stored at −80°C for further experiments. The complete metabolic profile during development and ripening shown in this work corresponds to fruits collected during 2008. Fruits collected during 2005 and 2010 were also analyzed for metabolite composition at harvest (H).

Protein Extraction for Activity Measurements

Total protein from different peach fruit samples was extracted using buffer containing 400 mM Tris-HCl, pH 8.5, 5 mM EDTA, 10 mM $MgCl_2$, 10 mM β-mercaptoethanol, 20% (v/v) glycerol, 10 mM ascorbic acid, 1 mM phenylmethylsulfonyl fluoride, and 1% (v/v) Triton X-100 in a ratio of buffer to fresh tissue weight of 0.3 mL to 1 g. Thirty-three microliters of protease inhibitor cocktail (Sigma) was used per gram of fresh tissue. In the case of the crude extract prepared for invertase measurements, 400 mM HEPES-NaOH, pH 8.5, was used instead of Tris-HCl, pH 8.5. In all cases, samples were completely ground in a cold mortar with the addition of insoluble polyvinyl polypyrrolidone (Sigma) and centrifuged at 10,000*g* for 15 min at 4°C. Crude extract supernatants were desalted, according to Penefsky (1977), in a cold Sephadex G-25 column preequilibrated with a buffer of the same composition as the extraction buffer but containing 100 mM Tris-HCl, pH 8.0, or 100 mM HEPES-NaOH, pH 8.0. These crude extracts were used for activity and protein measurements.

Protein Quantification

Protein concentration was determined by the method of Bradford (1976) using the Bio-Rad protein assay reagent and bovine serum albumin as a standard.

Enzyme Assay

Enzyme activity was measured spectrophotometrically in a final volume of 1 mL at 30°C and 340 nm using a Helios β-spectrophotometer (UNICAM Instruments). Reaction mixtures used for each enzyme were as follows.

Invertases

NI activity was assayed in an incubation mixture containing 200 mM HEPES-NaOH, pH 7.5, 250 mM Suc, and an aliquot of the protein extract to be tested. The mixture was incubated at 30°C for different times, and reaction process was followed to detect the amount of Glc produced by using the Glc oxidase/horseradish peroxidase assay. AI was assayed in the conditions described above, although the reaction mixture contained 100 mM acetic acid/sodium acetate buffer, pH 5.0, and 25 mM Suc. In the case of AI, the aliquot was neutralized prior to Glc determination (Vargas et al., 2007).

PEPC

For PEPC, 100 mM Tris-HCl, pH 8.0, 20% (v/v) glycerol, 10 mM $MgCl_2$, 10 mM $NaHCO_3$, 4 mM PEP, 0.15 mM NADH, and 10 units of malate dehydrogenase (Lara et al., 2003) were used.

NADP-ME

For NADP-ME, 50 mM Tris-HCl, pH 7.5, 0.5 mM NADP, 10 mM L-malate, and 10 mM $MgCl_2$ were used. Reaction was started by the addition of malate (Detarsio et al., 2003).

NAD-ME

For NAD-ME, 50 mM HEPES, pH 7.3, 2 mM NAD, 2 mM L-malate, 5 mM dithiothreitol, 75 μM CoA, 5 mM $MgCl_2$, 5 mM $MnCl_2$, and 10 units of malate dehydrogenase were used. After the rapid increase of the A_{340}, the subsequent steady increase is attributable to the decarboxylation of L-malate by NAD-ME (Tronconi et al., 2008).

RNA Isolation and RT-PCR

Total RNA from different peach samples was isolated employing 4 g of tissue using the method described by Meisel et al. (2005). RNA integrity was verified by agarose electrophoresis and by isolation and sequence determination of the complete coding sequences for some known transcripts. RNA quantity and purity were determined spectrophotometrically. First-strand cDNA was synthesized with Moloney murine leukemia virus reverse transcriptase following the manufacturer's instructions (Promega) and using 3 μg of RNA and oligo(dT).

qRT-PCR

Relative expression was determined by performing qRT-PCR in an iCycler iQ detection system and Optical System Software version 3.0a (Bio-Rad), using the intercalation dye SYBR Green I (Invitrogen) as a fluorescence reporter, with 2.5 mM $MgCl_2$, 0.5 μM of each primer, and 0.04 units μL^{-1} GoTaq Polymerase (Promega). PCR primers were designed based on peach fruit cDNA sequences published in GenBank and peach EST databases (The Institute for Genomic Research Plant Transcript Assemblies; http://plantta.jcvi.org [Childs et al., 2007]), with the aid of the Web-based program primer3 (http://frodo.wi.mit.edu/primer3/), to produce amplicons of 131 to 234 bp in size (Supplemental Table S3). Primer and amplicon sequences were further analyzed using peach EST databases (ESTree; http://www.itb.cnr.it/estree/ [Lazzari et al., 2008] and the Genome Database for Rosaceae; http://www.bioinfo.wsu.edu/gdr/ [Jung et al., 2008]). A 10-fold dilution of cDNA obtained as described above was used as template. PCR controls were performed in the absence of added reverse transcriptase to ensure DNA-free RNA samples. Cycling parameters were as follows: initial denaturation at 94°C for 2 min; 35 cycles at 96°C for 10 s, 58°C for 15 s, 72°C for 1 min, and 72°C for 10 min. Melting curves for each PCR were monitored by measuring fluorescence quenching with increasing temperature (from 65°C to 98°C). PCR specificity was confirmed by software-based melting curve analysis as well as by agarose gel electrophoresis of the products. Relative gene expression was calculated using the comparative $2^{-\Delta\Delta CT}$ method (Livak and Schmittgen, 2001) and elongation factor-1α from peach (*EF-1α*; Supplemental Table S3) as a reference gene. Each assay was run in triplicate and repeated at least three times using different samples.

Metabolite Measurements

Metabolite analysis by GC-MS was carried out essentially as described by Roessner-Tunali et al. (2003). Whole fruit (for E samples) or representative mesocarp tissue of peach fruits (250 mg) at different development stages (S1–S4) and during the ripening process (H–H7) were ground using ceramic mortar and pestle precooled with liquid nitrogen and extracted in 3 mL of methanol. Internal standard (180 μL; 0.2 mg ribitol mL^{-1} MilliQ water) was subsequently added for quantification purposes. The mixture was extracted for 15 min at 70°C (vortexing every 3 min) and mixed vigorously with precooled MilliQ water (1.5 mL). After centrifugation at 2,200*g*, an aliquot of

the supernatant (50 μL) was transferred to a reaction tube (1.5 mL) and vacuum dried. Tubes were filled with argon gas and stored at −80°C. Samples were derivatized and GC-MS was performed as described by Roessner-Tunali et al. (2003). Mass spectra were cross-referenced with those in the Golm Metabolome Database (Kopka et al., 2005). Five independent determinations, composed of three different fruits of the same stage, were performed for each sample analyzed. Data presented are normalized to the harvest peach fruit (H) and expressed as $\log_2$ ratios to H using the MultiExperiment Viewer software (version 4.4.1; http://www.tm4.org/ [Saeed et al., 2003]). Determination of the absolute concentrations of identified metabolites was performed by comparison with calibration standard curve response ratios of various concentrations of standard solutions, including the internal standard ribitol, which were derivatized concomitantly to tissue samples.

Principal component analysis was performed on data sets obtained from metabolite profiling by employing the software package TMEV (Saeed et al., 2003) and applying the default weighted covariance estimation function. The data were $\log_2$ transformed and normalized to the median of the entire sample set for each metabolite before analysis. Correlation analysis between metabolites based on Pearson correlation was performed using R software (Ihaka and Gentleman, 1996).

Sorbitol was determined enzymatically using SDH from sheep (Sigma) according to Bergmeyer et al. (1974). Samples were ground in a mortar with liquid N_2 and deproteinized with perchloric acid in order to prevent further conversion of sorbitol by endogenous enzymes (Bergmeyer et al., 1974). A calibration curve with known sorbitol concentrations was performed.

Statistical Analysis

Data presented were analyzed using one-way ANOVA. Minimum significance differences were calculated by the Bonferroni, Holm-Sidak, Dunnett, and Duncan tests ($\alpha = 0.05$) using the SigmaStat Package.

Supplemental Data

The following materials are available in the online version of this article.

Supplemental Table S1. Levels of 47 metabolites relative to their amount found in harvest peach fruits (H), and ANOVA *P* values expressing the statistical significance of changes in primary metabolite content across developmental stages and ripening.

Supplemental Table S2. Quantitative determination of the concentrations of 21 metabolites identified in peach cv Dixiland mesocarp at H.

Supplemental Table S3. Oligonucleotide sequences of primers used for real-time RT-PCR analysis.

ACKNOWLEDGMENTS

M.F.D., M.V.L., C.A.B., and C.S.A. are members of the Researcher Career of Consejo Nacional de Investigaciones Científicas y Técnicas, and M.A.L. and J.B. are fellows of the same institution.

Received September 9, 2011; accepted October 19, 2011; published October 20, 2011.

LITERATURE CITED

Aranzana MJ, Abbassi K, Howad W, Arús P (2010) Genetic variation, population structure and linkage disequilibrium in peach commercial varieties. BMC Genet **11:** 69

Araújo WL, Ishizaki K, Nunes-Nesi A, Larson TR, Tohge T, Krahnert I, Witt S, Obata T, Schauer N, Graham IA, et al (2010) Identification of the 2-hydroxyglutarate and isovaleryl-CoA dehydrogenases as alternative electron donors linking lysine catabolism to the electron transport chain of *Arabidopsis* mitochondria. Plant Cell **22:** 1549–1563

Bergmeyer HU, Gruber W, Gutmann I (1974). D-Sorbitol. *In* HU Bergmeyer, ed, Methods of Enzymatic Analysis, Ed 2, Vol III. Academic Press, New York, pp 1323–1330

Bernal-Lugo I, Leopold AC (1995) Seed stability during storage: raffinose content and seed glassy state. Seed Sci Res **5:** 75–80

Borsani J, Budde CO, Porrini L, Lauxmann MA, Lombardo VA, Murray R, Andreo CS, Drincovich MF, Lara MV (2009) Carbon metabolism of peach fruit after harvest: changes in enzymes involved in organic acid and sugar level modifications. J Exp Bot **60:** 1823–1837

Bradford MM (1976) A rapid and sensitive method for the quantitation of microgram quantities of protein utilizing the principle of protein-dye binding. Anal Biochem **72:** 248–254

Budde CO, Polenta G, Lucangeli CD, Murray RE (2006) Air immersion heat treatments affect ethylene production and organoleptic quality of 'Dixiland' peaches. Postharvest Biol Technol **41:** 32–37

Carrari F, Baxter C, Usadel B, Urbanczyk-Wochniak E, Zanor MI, Nunes-Nesi A, Nikiforova V, Centero D, Ratzka A, Pauly M, et al (2006) Integrated analysis of metabolite and transcript levels reveals the metabolic shifts that underlie tomato fruit development and highlight regulatory aspects of metabolic network behavior. Plant Physiol **142:** 1380–1396

Carrari F, Fernie AR (2006) Metabolic regulation underlying tomato fruit development. J Exp Bot **57:** 1883–1897

Chalmers DJ, van den Ende B (1975) A reappraisal of the growth and development of peach fruit. Aust J Plant Physiol **2:** 623–634

Childs KL, Hamilton JP, Zhu W, Ly E, Cheung F, Wu H, Rabinowicz PD, Town CD, Buell CR, Chan AP (2007) The TIGR plant transcript assemblies database. Nucleic Acids Res **35:** D846–D851

Dardick CD, Callahan AM, Chiozzotto R, Schaffer RJ, Piagnani MC, Scorza R (2010) Stone formation in peach fruit exhibits spatial coordination of the lignin and flavonoid pathways and similarity to Arabidopsis dehiscence. BMC Biol **8:** 13

Deluc LG, Grimplet J, Wheatley MD, Tillett RL, Quilici DR, Osborne C, Schooley DA, Schlauch KA, Cushman JC, Cramer GR (2007) Transcriptomic and metabolite analyses of Cabernet Sauvignon grape berry development. BMC Genomics **8:** 429

Detarsio E, Wheeler MC, Campos Bermúdez VA, Andreo CS, Drincovich MF (2003) Maize C4 NADP-malic enzyme: expression in Escherichia coli and characterization of site-directed mutants at the putative nucleoside-binding sites. J Biol Chem **278:** 13757–13764

Dirlewanger E, Cosson P, Bouderhi K, Renaud C, Capdeville G, Tauzin Y, Laigret F, Moing A (2006) Development of a second-generation genetic linkage map for peach [*Prunus persica* (L.) Batsch] and characterization of morphological traits affecting flower and fruit. Tree Genet Genomes **3:** 1–13

Downie B, Bewley JD (2000) Soluble sugar content of white spruce (*Picea glauca*) seeds during and after germination. Physiol Plant **110:** 1–12

El-Sharkawy I, Kim WS, El-Kereamy A, Jayasankar S, Svircev AM, Brown DCW (2007) Isolation and characterization of four ethylene signal transduction elements in plums (*Prunus salicina* L.). J Exp Bot **58:** 3631–3643

Etienne C, Moing A, Dirlewanger E, Raymond P, Monet R, Rothan C (2002) Isolation and characterization of six peach cDNAs encoding key proteins in organic acid metabolism and solute accumulation: involvement in regulating peach fruit acidity. Physiol Plant **114:** 259–270

Fait A, Hanhineva K, Beleggia R, Dai N, Rogachev I, Nikiforova VJ, Fernie AR, Aharoni A (2008) Reconfiguration of the achene and receptacle metabolic networks during strawberry fruit development. Plant Physiol **148:** 730–750

Famiani F, Cultrera NGM, Battistelli A, Casulli V, Proietti P, Standardi A, Chen Z-H, Leegood RC, Walker RP (2005) Phosphoenolpyruvate carboxykinase and its potential role in the catabolism of organic acids in the flesh of soft fruit during ripening. J Exp Bot **56:** 2959–2969

Fridman E, Carrari F, Liu YS, Fernie AR, Zamir D (2004) Zooming in on a quantitative trait for tomato yield using interspecific introgressions. Science **305:** 1786–1789

Giovannoni JJ (2004) Genetic regulation of fruit development and ripening. Plant Cell (Suppl) **16:** S170–S180

Horbowicz M, Obendorf RL (1994) Seed desiccation tolerance and storability: dependence of flatulence-producing oligosaccharides and cyclitols. Review and survey. Seed Sci Res **4:** 385–405

Ihaka R, Gentleman R (1996) R: a language for data analysis and graphics. J Comput Graph Statist **5:** 299–314

Ishizaki K, Schauer N, Larson TR, Graham IA, Fernie AR, Leaver CJ (2006) The mitochondrial electron transfer flavoprotein complex is essential for survival of Arabidopsis in extended darkness. Plant J **47:** 751–760

Jin Y, Ni D-A, Ruan Y-L (2009) Posttranslational elevation of cell wall

invertase activity by silencing its inhibitor in tomato delays leaf senescence and increases seed weight and fruit hexose level. Plant Cell **21:** 2072–2089

Jung S, Staton M, Lee T, Blenda A, Svancara R, Abbott A, Main D (2008) GDR (Genome Database for Rosaceae): integrated Web-database for Rosaceae genomics and genetics data. Nucleic Acids Res **36:** D1034–D1040

Kopka J, Schauer N, Krueger S, Birkemeyer C, Usadel B, Bergmüller E, Dörmann P, Weckwerth W, Gibon Y, Stitt M, et al (2005) GMD@CSB. DB: the Golm Metabolome Database. Bioinformatics **21:** 1635–1638

Lara MV, Borsani J, Budde CO, Lauxmann MA, Lombardo VA, Murray R, Andreo CS, Drincovich MF (2009) Biochemical and proteomic analysis of 'Dixiland' peach fruit (*Prunus persica*) upon heat treatment. J Exp Bot **60:** 4315–4333

Lara MV, Budde CO, Porrini L, Borsani J, Murray R, Andreo CS, Drincovich MF (2011) Peach (*Prunus persica*) fruit response to anoxia: reversible ripening delay and biochemical changes. Plant Cell Physiol **52:** 392–403

Lara MV, Disante K, Podestá FE, Andreo CS, Drincovich MF (2003) Induction of a Crassulacean acid-like metabolism in the C_4 succulent plant, *Portulaca oleracea* L.: physiological and morphological changes are accompanied by specific modifications in phosphoenolpyruvate carboxylase. Photosynth Res **77:** 241–254

Lazzari B, Caprera A, Vecchietti A, Merelli I, Barale F, Milanesi L, Stella A, Pozzi C (2008) Version VI of the ESTree db: an improved tool for peach transcriptome analysis. BMC Bioinformatics (Suppl 2) **9:** S9

Lin T-P, Huang N-H (1994) The relationship between carbohydrate composition of some tree seeds and their longevity. J Exp Bot **45:** 1289–1294

Livak KJ, Schmittgen TD (2001) Analysis of relative gene expression data using real-time quantitative PCR and the 2(-Δ Δ C(T)) method. Methods **25:** 402–408

Lo Bianco R, Rieger M, Sung S-JS (1999) Carbohydrate metabolism of vegetative and reproductive sinks in the late-maturing peach cultivar 'Encore'. Tree Physiol **19:** 103–109

Luo J, Butelli E, Hill L, Parr A, Niggeweg R, Bailey P, Weisshaar B, Martin C (2008) AtMYB12 regulates caffeoyl quinic acid and flavonol synthesis in tomato: expression in fruit results in very high levels of both types of polyphenol. Plant J **56:** 316–326

Macheix JJ, Sapis JC, Fleuriet A (1991) Phenolic compounds and polyphenoloxidase in relation to browning in grapes and wines. Crit Rev Food Sci Nutr **30:** 441–486

Meisel L, Fonseca B, González S, Baeza-Yates R, Cambiazo V, Campos R, Gonźalez M, Orellana A, Retamales J, Silva H (2005) A rapid and efficient method for purifying high quality total RNA from peaches (*Prunus persica*) for functional genomics analyses. Biol Res **38:** 83–88

Moing A, Carbonne F, Zipperlin B, Svanella L, Gaudillere JP (1997) Phloem loading in peach: symplastic or apoplastic? Physiol Plant **101:** 489–496

Moing A, Savanella L, Rolin D, Gaudeillere M, Guadillere JP, Monet R (1998) Compositional changes during the fruit development of two peach cultivars differing in juice acidity. J Am Soc Hortic Sci **123:** 770–775

Nadwodnik J, Lohaus G (2008) Subcellular concentrations of sugar alcohols and sugars in relation to phloem translocation in Plantago major, Plantago maritima, Prunus persica, and Apium graveolens. Planta **227:** 1079–1089

Osorio S, Bombarely A, Giavalisco P, Usadel B, Stephens C, Aragüez I, Medina-Escobar N, Botella MA, Fernie AR, Valpuesta V (2011) Demethylation of oligogalacturonides by FaPE1 in the fruits of the wild strawberry *Fragaria vesca* triggers metabolic and transcriptional changes associated with defence and development of the fruit. J Exp Bot **62:** 2855–2873

Penefsky HS (1977) Reversible binding of Pi by beef heart mitochondrial adenosine triphosphatase. J Biol Chem **252:** 2891–2899

Roby C, Cortès S, Gromova M, Le Bail J-L, Roberts JKM (2002) Sucrose cycling in heterotrophic plant cell metabolism: first step towards an experimental model. Mol Biol Rep **29:** 145–149

Roessner-Tunali U, Hegemann B, Lytovchenko A, Carrari F, Bruedigam C, Granot D, Fernie AR (2003) Metabolic profiling of transgenic tomato plants overexpressing hexokinase reveals that the influence of hexose phosphorylation diminishes during fruit development. Plant Physiol **133:** 84–99

Roitsch T, González M-C (2004) Function and regulation of plant invertases: sweet sensations. Trends Plant Sci **9:** 606–613

Ruperti B, Bonghi C, Rasori A, Ramina A, Tonutti P (2001) Characterization and expression of two members of the peach 1-aminocyclopropane-1-carboxylate oxidase gene family. Physiol Plant **111:** 336–344

Saeed AI, Sharov V, White J, Li J, Liang W, Bhagabati N, Braisted J, Klapa M, Currier T, Thiagarajan M, et al (2003) TM4: a free, open-source system for microarray data management and analysis. Biotechniques **34:** 374–378

Shulaev V, Korban SS, Sosinski B, Abbott AG, Aldwinckle HS, Folta KM, Iezzoni A, Main D, Arús P, Dandekar AM, et al (2008) Multiple models for Rosaceae genomics. Plant Physiol **147:** 985–1003

Swanson CA (1998) Vegetables, fruits, and cancer risk: the role of phytochemicals. *In* WR Bidlack, ST Omaye, MS Meskin, DKW Topham, eds, Phytochemicals: A New Paradigm. CRC Press, Boca Raton, FL, pp 1–12

Taji T, Ohsumi C, Iuchi S, Seki M, Kasuga M, Kobayashi M, Yamaguchi-Shinozaki K, Shinozaki K (2002) Important roles of drought- and cold-inducible genes for galactinol synthase in stress tolerance in Arabidopsis thaliana. Plant J **29:** 417–426

Tonutti P, Bonghi C, Ruperti B, Tornielli GB, Ramina A (1997) Ethylene evolution and 1-aminocyclopropane-1-carboxylate oxidase gene expression during early development and ripening of peach fruit. J Am Soc Hortic Sci **122:** 642–647

Tonutti P, Casson P, Ramina A (1991) Ethylene biosynthesis during peach fruit development. J Am Soc Hortic Sci **116:** 274–279

Trainotti L, Tadiello A, Casadoro G (2007) The involvement of auxin in the ripening of climacteric fruits comes of age: the hormone plays a role of its own and has an intense interplay with ethylene in ripening peaches. J Exp Bot **58:** 3299–3308

Trainotti L, Zanin D, Casadoro G (2003) A cell wall-oriented genomic approach reveals a new and unexpected complexity of the softening in peaches. J Exp Bot **54:** 1821–1832

Tronconi MA, Fahnenstich H, Gerrard Weehler MC, Andreo CS, Flügge U-I, Drincovich MF, Maurino VG (2008) Arabidopsis NAD-malic enzyme functions as a homodimer and heterodimer and has a major impact on nocturnal metabolism. Plant Physiol **146:** 1540–1552

van der Merwe MJ, Groenewald J-H, Stitt M, Kossmann J, Botha FC (2010) Downregulation of pyrophosphate:D-fructose-6-phosphate 1-phosphotransferase activity in sugarcane culms enhances sucrose accumulation due to elevated hexose-phosphate levels. Planta **231:** 595–608

Vargas WA, Pontis HG, Salerno GL (2007) Differential expression of alkaline and neutral invertases in response to environmental stresses: characterization of an alkaline isoform as a stress-response enzyme in wheat leaves. Planta **226:** 1535–1545

Vargas WA, Pontis HG, Salerno GL (2008) New insights on sucrose metabolism: evidence for an active A/N-Inv in chloroplasts uncovers a novel component of the intracellular carbon trafficking. Planta **227:** 795–807

Vargas WA, Salerno GL (2010) The Cinderella story of sucrose hydrolysis: alkaline/neutral invertases, from cyanobacteria to unforeseen roles in plant cytosol and organelles. Plant Sci **178:** 1–8

Weigelt K, Küster H, Radchuk R, Müller M, Weichert H, Fait A, Fernie AR, Saalbach I, Weber H (2008) Increasing amino acid supply in pea embryos reveals specific interactions of N and C metabolism, and highlights the importance of mitochondrial metabolism. Plant J **55:** 909–926

Yativ M, Harary I, Wolf S (2010) Sucrose accumulation in watermelon fruits: genetic variation and biochemical analysis. J Plant Physiol **167:** 589–596

Zamboni A, Di Carli M, Guzzo F, Stocchero M, Zenoni S, Ferrarini A, Tononi P, Toffali K, Desiderio A, Lilley KS, et al (2010) Identification of putative stage-specific grapevine berry biomarkers and omics data integration into networks. Plant Physiol **154:** 1439–1459

Zanor MI, Osorio S, Nunes-Nesi A, Carrari F, Lohse M, Usadel B, Kühn C, Bleiss W, Giavalisco P, Willmitzer L, et al (2009) RNA interference of LIN5 in tomato confirms its role in controlling Brix content, uncovers the influence of sugars on the levels of fruit hormones, and demonstrates the importance of sucrose cleavage for normal fruit development and fertility. Plant Physiol **150:** 1204–1218

Ziosi V, Bregoli AM, Fregola F, Costa G, Torrigiani P (2009) Jasmonate-induced ripening delay is associated with up-regulation of polyamine levels in peach fruit. J Plant Physiol **166:** 938–946